

Perturbation theory for the redshift-space matter power spectra after reconstruction

Chiaki Hikage

*Kavli Institute for the Physics and Mathematics of the Universe (Kavli IPMU,
WPI), University of Tokyo, 5-1-5 Kashiwanoha, Kashiwa, Chiba, 277-8583, Japan*

Kazuya Koyama

Institute of Cosmology and Gravitation, University of Portsmouth, Portsmouth PO1 3FX, UK

Ryuichi Takahashi

*Faculty of Science and Technology, Hirosaki University,
3 Bunkyo-cho, Hirosaki, Aomori 036-8588, Japan*

(Dated: February 19, 2024)

We derive the one-loop perturbative formula of the redshift-space matter power spectrum after density field reconstruction in the Zeldovich approximation. We find that the reconstruction reduces the amplitudes of nonlinear one-loop perturbative terms significantly by partially erasing the nonlinear mode-coupling between density and velocity fields. In comparison with N-body simulations, we find that both the monopole and quadrupole spectra of reconstructed matter density fields agree with the one-loop perturbation theory up to higher wavenumber than those before reconstruction. We also evaluate the impact on cosmic growth rate assuming the survey volume and the number density like the Baryon Oscillation Spectroscopic Survey and find that the total error, including statistical and systematic ones due to one-loop approximation, decreases by half.

I. INTRODUCTION

Large-scale structure in the Universe is a powerful cosmological probe to understand the properties of dark matter and dark energy [e.g., 1]. Baryonic Acoustic Oscillations (BAO) imprinted on the large-scale structure plays a role as a standard ruler [2–12] to determine the expansion history of the Universe from various galaxy surveys [13–24]. The overall shape of the matter power spectrum is useful to infer the neutrino mass [25, 26]. The anisotropy in the redshift-space clustering due to the bulk motion of galaxies provides a key probe to test General Relativity [e.g., 27–33]. One can expect precision cosmological analysis from galaxy clustering in upcoming galaxy surveys such as the Prime Focus Spectrograph (PFS) [34], the Dark Energy Spectroscopic Instrument (DESI) [35], the Hobby-Eberly Telescope Dark Energy Experiment (HETDEX) [36], Euclid [37], the Wide Field Infrared Survey Telescope (WFIRST) [38].

Nonlinearity in the gravitational evolution of large-scale structure makes precise cosmological analysis complicated. The BAO feature is degraded with structure formation mainly due to the bulk motions of matter [e.g., 39]. The perturbation theory has been derived to describe the nonlinear effects on the power spectra [e.g., 40–49], however, the availability is limited to the weakly nonlinear regime even including the higher-order nonlinear terms [50–55]. Evolved density fields no longer follow Gaussian statistics and thereby their clustering information is not fully described with two-point statistics but leaks to higher-order statistics.

Eisenstein et al. [56] applies a density field reconstruction technique to aim for recovering the original BAO signature by undoing the bulk motion in the Zeldovich approximation [57]. The method has been extensively studied analytically and tested using numerical simulations [58–62] and applied to the current BAO analysis [18–24, 63]. It is also shown that the density field reconstruction recover the initial density field out to smaller scales using more optimal ways of density field reconstruction beyond the standard reconstruction method [61, 64–70].

Although the reconstruction succeeds in the BAO analysis, it is relatively unclear how the reconstructed power spectrum can be described in a perturbative manner. In this paper, we derive the exact one-loop order perturbative formula of the redshift-space matter power spectra after reconstruction. In our previous work, we derive the one-loop perturbative formula of real-space matter power spectra and find that the amplitudes of the one-loop terms decrease significantly and then the perturbation theory can be applied to higher wavenumber k . The result is consistent with the previous work showing that the reconstructed field better recovers the initial density field [e.g., 61]. In this paper, we extend our previous work to redshift-space matter density fields. Recently Chen et al. [71] presented the perturbative formula of halo power spectra in redshift space. Our analysis is limited to the matter power spectra in redshift space, but include the nonlinearities from the Lagrangian to Eulerian mapping in our perturbative formula. From the comparison with large-scale suite of N-body simulations, we study to what extent the monopole and quadrupole spectra of the redshift-space matter fields can be described in one-loop order. We also demonstrate the impact on the cosmic growth rate assuming the survey volume and the number density like the Baryon Oscillation Spectro-

* chiaki.hikage@ipmu.jp

scopic Survey (BOSS) [23] when modeling the redshift-space power spectra with the one-loop perturbation.

The paper is organized as follows: Section II describes the one-loop perturbation theory of the redshift-space matter power spectra and explicitly show the one-loop results in the Appendix A. In Section III, we study how the one-loop perturbation better describes the redshift-space matter power spectra in comparison with N-body simulations. Section IV is devoted to summary and conclusions.

II. ONE-LOOP STANDARD PERTURBATION THEORY OF REDSHIFT-SPACE MATTER POWER SPECTRA

In this section, we derive the perturbative formula based on the standard perturbation theory (SPT) to describe the nonlinearity in the redshift-space matter power spectrum at one-loop order.

The comoving redshift space-position \mathbf{x} is related to the Lagrangian position \mathbf{q} as

$$\mathbf{x} = \mathbf{q} + \Psi^z(\mathbf{q}), \quad (1)$$

where Ψ^z is the comoving displacement in redshift space given by

$$\Psi^z = \Psi + \frac{\hat{\mathbf{z}} \cdot \dot{\Psi}}{H} \hat{\mathbf{z}}, \quad (2)$$

where H is the time-dependent Hubble parameter and $\hat{\mathbf{z}}$ is the unit vector of the line-of-sight direction. In the Einstein-de-Sitter (EdS) model, the n -th order perturbative displacement $\Psi^{(n)}$ is proportional to n -th power of the linear growth factor D and thereby the time derivative of the displacement becomes

$$\dot{\Psi}^{(n)} = nHf\Psi^{(n)}, \quad (3)$$

where $f = d\ln D/d\ln a$ is the linear growth rate. In a Λ CDM cosmology, the EdS approximation is valid to less than a percent level at the one-loop order of power spectra on the scales of our interest [72–75]. The n -th order displacement in redshift space then becomes

$$\Psi^{z(n)} = \mathbf{R}^{(n)}\Psi^{(n)}, \quad (4)$$

where

$$\mathbf{R}_{ij}^{(n)} = \delta_{ij} + nf\hat{z}_i\hat{z}_j, \quad (5)$$

and δ_{ij} is Kronecker delta. The perturbative kernels in redshift space is given by

$$\mathbf{L}^{z(n)} = \mathbf{R}^{(n)}\mathbf{L}^{(n)}. \quad (6)$$

The shift field $\mathbf{s}_z(\mathbf{x})$ in redshift space is computed from the negative ZA [57] of the smoothed density field as

$$\mathbf{s}^z(\mathbf{x}) = \int \frac{d\mathbf{k}}{(2\pi)^3} \tilde{\mathbf{s}}_k^z e^{i\mathbf{k}\cdot\mathbf{x}}, \quad (7)$$

$$\tilde{\mathbf{s}}_k^z = -iW(k)\mathbf{L}^{(1)}(\mathbf{k})\tilde{\delta}_k^z, \quad (8)$$

where $W(k)$ is the smoothing kernel and we adopt a Gaussian kernel $W(k) = \exp(-k^2 R_s^2/2)$ with the smoothing scale of R_s . We found that the perturbation works best around $R_s = 10h^{-1}\text{Mpc}$ in real space[76] and thereby we fix R_s to be $10h^{-1}\text{Mpc}$ in this paper. The perturbative series of the shift field is given by

$$\tilde{\mathbf{s}}_k^{z(n)} = -iW(k)\mathbf{L}^{(1)}(\mathbf{k})\tilde{\delta}_k^{z(n)}. \quad (9)$$

where $\tilde{\delta}_k^{z(n)}$ is the n -th order perturbation of the redshift-space density fluctuation. This can be rewritten as

$$\tilde{\mathbf{s}}_k^{z(n)} = \frac{iD^n}{n!} \int \frac{d\mathbf{k}_1 \cdots d\mathbf{k}_n}{(2\pi)^{3n-3}} \delta_D \left(\sum_{j=1}^n \mathbf{k}_j - \mathbf{k} \right) \times \mathbf{S}^{z(n)}(\mathbf{k}_1, \dots, \mathbf{k}_n) \tilde{\delta}_{\mathbf{k}_1}^L \cdots \tilde{\delta}_{\mathbf{k}_n}^L, \quad (10)$$

where the kernel of the shift field $\mathbf{S}^{z(n)}$ is written with the redshift-space Eulerian kernel F_n^z as

$$\mathbf{S}^{z(n)}(\mathbf{k}_1, \dots, \mathbf{k}_n) = -n!W(k)\mathbf{L}^{(1)}(\mathbf{k})F_n^z(\mathbf{k}_1, \dots, \mathbf{k}_n). \quad (11)$$

The redshift-space kernel is given in the previous literature [e.g., 50, 77, 78]:

$$F_1^z = 1 + f\mu^2, \quad (12)$$

$$F_2^z(\mathbf{k}_1, \mathbf{k}_2) = F_2(\mathbf{k}_1, \mathbf{k}_2) + f\mu^2 G_2(\mathbf{k}_1, \mathbf{k}_2) + \frac{1}{2}fk\mu \left(\frac{k_{1z}}{k_1^2} + \frac{k_{2z}}{k_2^2} \right) + \frac{1}{2}(fk\mu)^2 \frac{k_{1z}k_{2z}}{k_1^2 k_2^2}, \quad (13)$$

$$\begin{aligned} F_3^z(\mathbf{k}_1, \mathbf{k}_2, \mathbf{k}_3) &= F_3(\mathbf{k}_1, \mathbf{k}_2, \mathbf{k}_3) + f\mu^2 G_3(\mathbf{k}_1, \mathbf{k}_2, \mathbf{k}_3) \\ &\quad + fk\mu \frac{k_{1z}}{k_1^2} F_2(\mathbf{k}_2, \mathbf{k}_3) \\ &\quad + fk\mu \frac{k_{2z} + k_{3z}}{|\mathbf{k}_2 + \mathbf{k}_3|^2} G_2(\mathbf{k}_2, \mathbf{k}_3) \\ &\quad + (fk\mu)^2 \frac{k_{1z}(k_{2z} + k_{3z})}{k_1^2 |\mathbf{k}_2 + \mathbf{k}_3|^2} G_2(\mathbf{k}_2, \mathbf{k}_3) \\ &\quad + \frac{1}{2}(fk\mu)^2 \frac{k_{1z}k_{2z}}{k_1^2 k_2^2} + \frac{1}{6}(fk\mu)^3 \frac{k_{1z}k_{2z}k_{3z}}{k_1^2 k_2^2 k_3^2}, \end{aligned} \quad (14)$$

where $\mu = \mathbf{k} \cdot \hat{\mathbf{z}}/k$ and G_n is the n -th kernel of peculiar velocity field.

The displaced density field is written as

$$\tilde{\delta}_k^{z(d)} = \int d\mathbf{q} e^{-i\mathbf{k}\cdot\mathbf{q}} (e^{-i\mathbf{k}\cdot[\Psi^z(\mathbf{q}) + \mathbf{s}^z(\mathbf{x})]} - 1), \quad (15)$$

where the shift field of the evolved mass particles is evaluated at the Eulerian positions \mathbf{x} . The difference of the shift field between the Eulerian and Lagrangian positions

is perturbatively expanded in terms of Ψ as

$$\begin{aligned} \mathbf{s}^z(\mathbf{x}) &= \int \frac{d\mathbf{k}}{(2\pi)^3} \tilde{\mathbf{s}}_{\mathbf{k}}^z e^{i\mathbf{k}\cdot(\mathbf{q}+\Psi^z(\mathbf{q}))}, \\ &= \sum_{n=0}^{\infty} \int \frac{d\mathbf{k}}{(2\pi)^3} \tilde{\mathbf{s}}_{\mathbf{k}}^z e^{i\mathbf{k}\cdot\mathbf{q}} \left[\frac{1}{n!} (i\mathbf{k}\cdot\Psi^z(\mathbf{q}))^n \right], \\ &= \mathbf{s}^z(\mathbf{q}) + (\Psi^z(\mathbf{q}) \cdot \nabla) \mathbf{s}^z(\mathbf{q}) + \frac{1}{2} (\Psi^z(\mathbf{q}) \cdot \nabla)^2 \mathbf{s}^z(\mathbf{q}) \dots \end{aligned}$$

The shifted density field of a spatially uniform grid or random is given by

$$\tilde{\delta}_{\mathbf{k}}^{z(s)} = \int d\mathbf{q} e^{-i\mathbf{k}\cdot\mathbf{q}} (e^{-i\mathbf{k}\cdot\mathbf{s}^z(\mathbf{q})} - 1), \quad (18)$$

where the shift field of the (unevolved) uniform grid is evaluated at the Lagrangian position. The reconstructed density field in redshift space is given as

$$\begin{aligned} \tilde{\delta}_{\mathbf{k}}^{z(\text{rec})} &\equiv \tilde{\delta}_{\mathbf{k}}^{z(\text{d})} - \tilde{\delta}_{\mathbf{k}}^{z(s)} \\ &= \int d\mathbf{q} e^{-i\mathbf{k}\cdot\mathbf{q}} e^{-i\mathbf{k}\cdot\mathbf{s}^z(\mathbf{q})} (e^{-i\mathbf{k}\cdot[\Psi^z(\mathbf{q}) + \mathbf{s}^z(\mathbf{x}) - \mathbf{s}^z(\mathbf{q})]} - 1). \end{aligned} \quad (19)$$

The redshift-space formula is the same as that in real space but replacing the real-space kernels $\mathbf{L}^{(n)}$ and F_n with the redshift-space ones $\mathbf{L}^{z(n)}$ and F_n^z .

At linear order, the reconstructed density field in redshift space is not changed by reconstruction

$$\tilde{\delta}_{\mathbf{k}}^{z(\text{rec})(1)} = \delta_{\mathbf{k}}^{z(1)}. \quad (20)$$

Higher-order terms of $\delta^{(\text{rec})}$ are given by

$$\begin{aligned} \tilde{\delta}_{\mathbf{k}}^{z(\text{rec},n)} &= D^n(z) \int \frac{d\mathbf{k}_1 \cdots d\mathbf{k}_n}{(2\pi)^{3n-3}} \delta_D \left(\sum_{j=1}^n \mathbf{k}_j - \mathbf{k} \right) \\ &\times F_n^{z(\text{rec})}(\mathbf{k}_1, \dots, \mathbf{k}_n) \tilde{\delta}_{\mathbf{k}_1}^L \cdots \tilde{\delta}_{\mathbf{k}_n}^L \end{aligned} \quad (21)$$

where $F_n^{z(\text{rec})}$ is the Eulerian kernel for the reconstructed matter density field in redshift space. We have already derived the explicit form of the reconstructed Eulerian kernel in real space in the previous paper [76]. The first-order Eulerian kernel does not change after reconstruction

$$F_1^{z(\text{rec})} = F_1^z. \quad (22)$$

The second-order Eulerian kernel for the reconstructed field $F_2^{z(\text{rec})}$ can be derived by replacing the real-space kernel to the redshift-space one in the equation of (32) or (A10) in Hikage et al. [76] as

$$\begin{aligned} F_2^{z(\text{rec})}(\mathbf{k}_1, \mathbf{k}_2) &= F_2^z(\mathbf{k}_1, \mathbf{k}_2) \\ &+ \frac{1}{2} \left[(\mathbf{k} \cdot \mathbf{S}^{z(1)}(\mathbf{k}_1)) (\mathbf{k}_2 \cdot \mathbf{L}^{z(1)}(\mathbf{k}_2)) \right. \\ &\left. + (\mathbf{k} \cdot \mathbf{S}^{z(1)}(\mathbf{k}_2)) (\mathbf{k}_1 \cdot \mathbf{L}^{z(1)}(\mathbf{k}_1)) \right]. \end{aligned} \quad (23)$$

Note that $\mathbf{k}_i \cdot \mathbf{L}^{(1)}(\mathbf{k}_i)$ terms in the real space becomes unity and thereby they are not written explicitly in the real-space formula. In redshift space, however, $\mathbf{k}_i \cdot \mathbf{L}^{(1)}(\mathbf{k}_i)$ becomes $1 + f\mu_i^2$ where $\mu_i = \mathbf{k}_i \cdot \hat{\mathbf{z}}$ and thus the $F_2^{z(\text{rec})}(\mathbf{k}_1, \mathbf{k}_2)$ depends on the line-of-sight direction of the two wavenumbers \mathbf{k}_1 and \mathbf{k}_2 . This makes the one-loop perturbative formula complicated as shown in Appendix A.

The third-order kernel is also derived by replacing the real-space kernel with the redshift-space one in the equation of (33) or (A29) in [76] as

$$\begin{aligned} F_3^{z(\text{rec})}(\mathbf{k}_1, \mathbf{k}_2, \mathbf{k}_3) &= F_3^z(\mathbf{k}_1, \mathbf{k}_2, \mathbf{k}_3) \\ &+ \frac{1}{6} \left[2(\mathbf{k} \cdot \mathbf{S}^{z(1)}(\mathbf{k}_1)) F_2^z(\mathbf{k}_2, \mathbf{k}_3) \right. \\ &+ (\mathbf{k} \cdot \mathbf{S}^{z(1)}(\mathbf{k}_1)) (\mathbf{k} \cdot \mathbf{S}^{z(1)}(\mathbf{k}_2)) (\mathbf{k}_3 \cdot \mathbf{L}^{z(1)}(\mathbf{k}_3)) \\ &+ (\mathbf{k} \cdot \mathbf{S}^{z(2)}(\mathbf{k}_1, \mathbf{k}_2)) (\mathbf{k}_3 \cdot \mathbf{L}^{z(1)}(\mathbf{k}_3)) \\ &\left. + (2 \text{ perms.}) \right]. \end{aligned} \quad (24)$$

The third-order kernel also depends on the line-of-sight direction of three wavenumbers μ_i with $i = 1, 2$, and 3.

The reconstructed power spectrum at one-loop order is written by

$$P^{z(\text{rec}),1-\text{loop}}(k) = D^2(z) P_{11}^{z(\text{rec})}(k) + D^4(z) (P_{22}^{z(\text{rec})} + P_{13}^{z(\text{rec})}), \quad (25)$$

where $P_{nm}^{z(\text{rec})} = \langle \tilde{\delta}_{\mathbf{k}}^{(n)} \delta_{\mathbf{k}}^{(m)} \rangle$. The leading-order term is unchanged after reconstruction

$$P_{11}^{z(\text{rec})}(k, \mu) = (1 + f\mu^2)^2 P_L(k). \quad (26)$$

The one-loop terms of the redshift-space power spectrum can be written with the reconstructed Eulerian kernels as

$$P_{22}^{z(\text{rec})}(k, \mu) = 2 \int \frac{d\mathbf{p}}{(2\pi)^3} P_L(|\mathbf{k} - \mathbf{p}|) P_L(p) [F_2^{z(\text{rec})}(\mathbf{k} - \mathbf{p}, \mathbf{p})]^2, \quad (27)$$

and

$$P_{13}^{z(\text{rec})}(k, \mu) = 6 F_1^{z(\text{rec})}(k) P_L(k) \int \frac{d\mathbf{p}}{(2\pi)^3} P_L(p) F_3^{z(\text{rec})}(\mathbf{k}, \mathbf{p}, -\mathbf{p}). \quad (28)$$

The exact formula of the one-loop terms are summarized in Appendix A. The multipole components of the redshift-space power spectrum is generally obtained by the Legendre polynomial expansion as

$$P_\ell(k) = \frac{1}{2} \int_{-1}^1 d\mu P(k, \mu) \mathcal{L}_\ell(\mu), \quad (29)$$

where $\mathcal{L}_\ell(\mu)$ is the Legendre polynomials, for example, $\mathcal{L}_0(\mu) = 1$ and $\mathcal{L}_2(\mu) = (3\mu^2 - 1)/2$.

Figure 1 shows the k -dependence of the one-loop terms P_{13} and P_{22} in the monopole ($\ell = 0$) and quadrupole ($\ell = 2$) spectra before and after reconstruction. We find that the amplitudes of both one-loop terms significantly decrease after reconstruction in monopole and quadrupole spectra out to large k . This result is similar

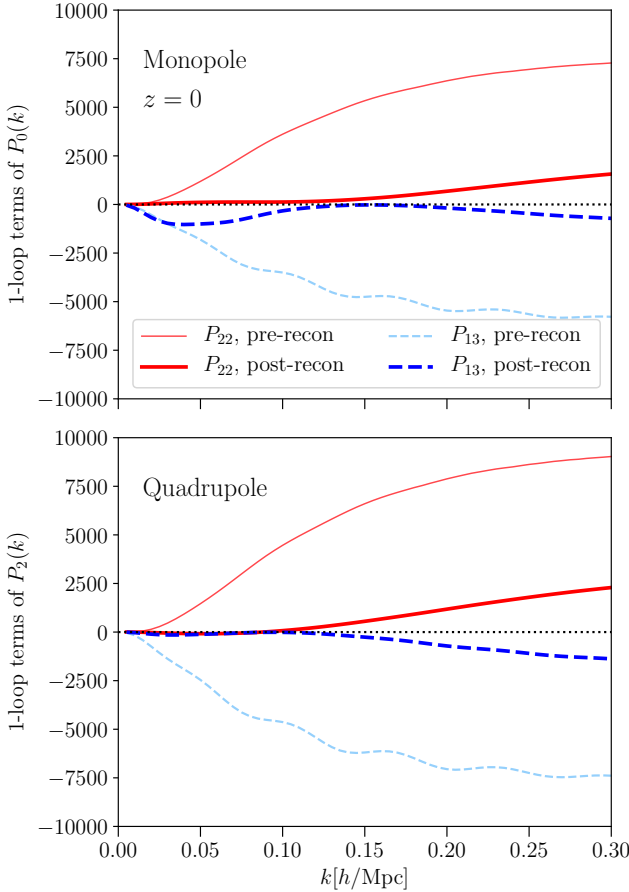


FIG. 1. Comparison of the one-loop terms $P_{22}(k)$ and $P_{13}(k)$ in monopole (upper) and quadrupole (lower) spectra of redshift-space matter density fields before (thin) and after (thick) reconstruction. The amplitudes of the both one-loop terms significantly decrease by reconstruction out to large k .

to the results in real space [cf. Fig. 1 of 76], but indicates that mode-couplings between density and velocity fields due to nonlinear gravity are partially removed by reconstruction. In-phase baryonic acoustic oscillations of P_{13} , but with negative amplitude, causes the degradation of the BAO signature. The oscillation of P_{13} also significantly reduces after reconstruction and thereby the original BAO signature is substantially recovered. The result is consistent with that the BAO feature in redshift-space spectra is actually recovered by the reconstruction [e.g., 63].

III. RESULTS

We compute the redshift-space matter power spectra using N -body simulations to see how well the one-loop perturbative formula describes the reconstructed spectra. Dark-matter N -body simulations are performed using a publicly available code **Gadget-2** [79]. The mass parti-

cles are initially distributed based on 2LPT code [80, 81] with Gaussian initial conditions at the input redshift of 31. The initial linear power spectrum is computed by CAMB [82]. Each simulation is performed in a cubic box with the side length of $4h^{-1}\text{Gpc}$ with 4096^3 particles. We assign the N -body particles to 2048^3 grid cells to calculate the density contrast, and then perform the Fourier transform [83] to measure the power spectrum. In our analysis, we use 8 realizations with two output redshifts of $z = 0$ and $z = 1.02$. We will show the average power spectrum with 1σ error estimated from these realizations. The cosmology in the simulations is based on a flat ΛCDM model with the best-fit values of Planck TT,TE,EE+lowP in 2015, i.e., $\Omega_b = 0.0492$, $\Omega_m = 0.3156$, $h = 0.6727$, $n_s = 0.9645$, and $\sigma_8 = 0.831$ [84].

We evaluate the agreement between the simulated power spectra and the perturbative formula with the following χ^2 value:

$$\chi^2 = \sum_i^{k_{\min} \leq k_i \leq k_{\max}} \sum_{\ell\ell'}^{0,2} [\mathbf{P}_\ell^{\text{theory}}(k_i) - \mathbf{P}_\ell^{\text{sim}}(k_i)] \mathbf{Cov}_{\ell\ell'}^{-1}(k_i) [\mathbf{P}_{\ell'}^{\text{theory}}(k_i) - \mathbf{P}_{\ell'}^{\text{sim}}(k_i)], \quad (30)$$

where $\mathbf{Cov}_{\ell\ell'}(k_i)$ represents the covariance of multipole power spectra at a given k_i . Here we focus on the monopole and quadrupole components of redshift-space matter power spectra. For simplicity, we adopt the analytical formula of the Gaussian covariance given by the Appendix C of Taruya et al. [52] with typos corrected and neglect the off-diagonal components of the covariance between different bins of k . This approximation would be valid when the cosmic variance and/or shot-noise terms are dominant compared to the non-Gaussian terms. The Gaussian covariance depends on the survey volume V and the number density n . In this paper, we assume BOSS-like survey with $V = 6(h^{-1}\text{Gpc})^3$ and $n = 2 \times 10^{-4}(h^{-1}\text{Mpc})^{-3}$. The chi-squared value depends on the range of k . Here we fix the minimum value $k_{\min} = 0.01h\text{Mpc}^{-1}$ and see how χ^2 changes as the maximum value k_{\max} increases. For the theoretical power spectrum $\mathbf{P}_\ell^{\text{theory}}(k)$, we adopt the one-loop perturbative formula with the lowest-order counter term proportional to $k^2 P_\ell$ in each ℓ

$$\mathbf{P}_\ell^{\text{theory}}(k) = \mathbf{P}_\ell^{\text{z,1-loop}}(k) + \alpha_\ell k^2 \mathbf{P}_\ell^{\text{L}}(k). \quad (31)$$

The counter terms renormalize the contributions from UV (small-scale) power [e.g., 85, 86] including the lowest-order contributions of nonlinear redshift-space distortions, i.e., Fingers-of-God effect. The proportional factor α_ℓ ($\ell = 0$ and 2) are obtained by fitted them to the simulated power spectra. Note that we adopt one counter term per each multipole for both pre-recon and post-recon spectrum, while [71] adopts three counter terms per each multipole proportional to the power spectra for $\langle \tilde{\delta}_k^{z(d)} \tilde{\delta}_k^{*z(d)} \rangle$, $\langle \tilde{\delta}_k^{z(d)} \tilde{\delta}_k^{*z(s)} \rangle$, $\langle \tilde{\delta}_k^{z(s)} \tilde{\delta}_k^{*z(s)} \rangle$ for the reconstructed spectrum.

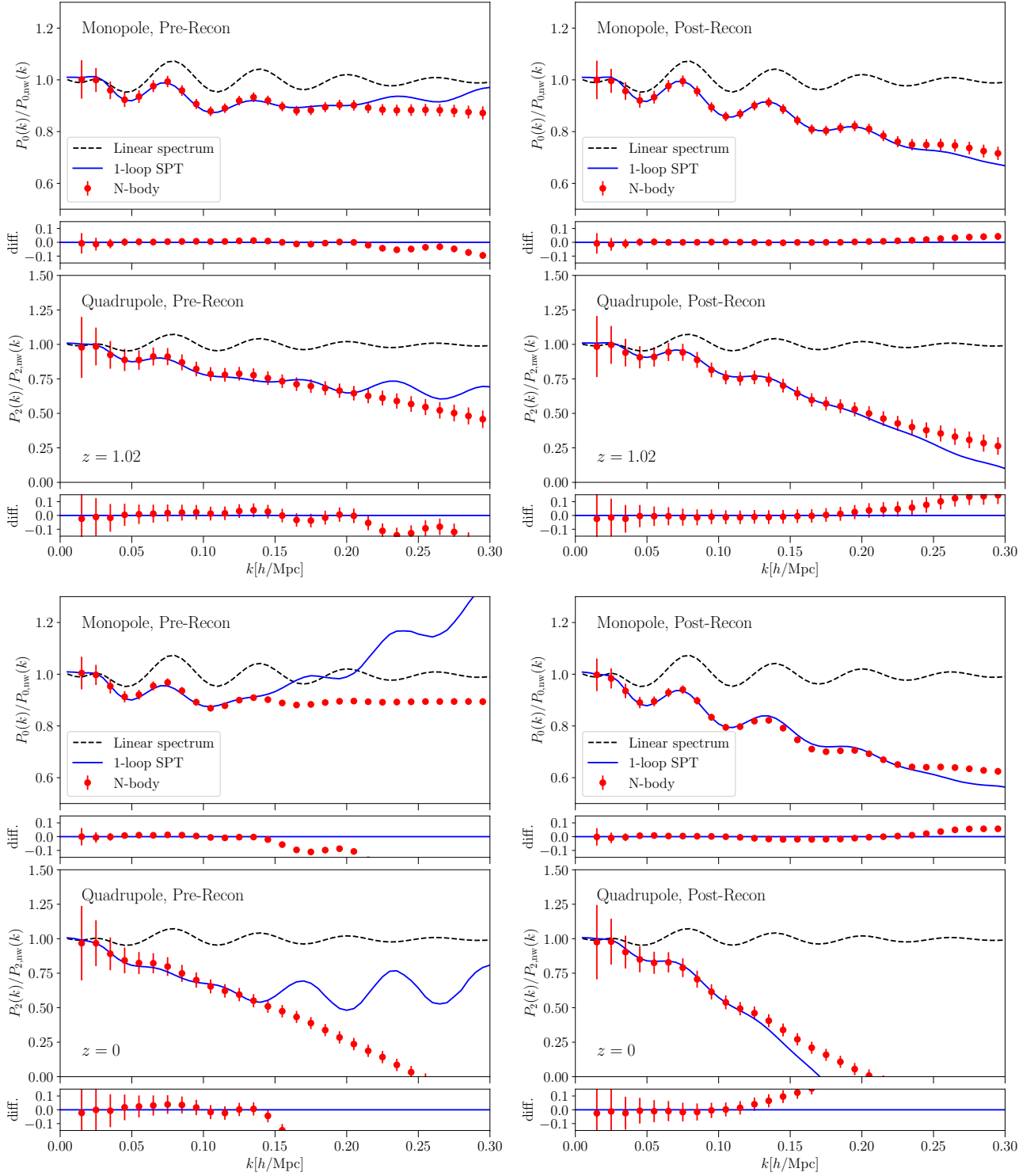


FIG. 2. Monopoles and quadrupoles of simulated redshift-space matter power spectrum (filled circles) before (left) and after (right) reconstruction at $z = 1.02$ (upper) and $z = 0$ (lower). For comparison, we plot the one-loop SPT (solid lines) with two counterterms proportional to $P_\ell^{(\text{lin})}(k)k^2$ fitted to the simulated spectra upto $k = 0.2h/\text{Mpc}$ for $z = 1.02$ and $k = 0.12h/\text{Mpc}$ for $z = 0$. For references, the linear spectra are plotted with lines. All of the power spectra are normalized with the no-wiggle multipole spectra in redshift space. The plotted error-bars are Gaussian error assuming a BOSS-like survey with the survey volume $V = 6(h^{-1}\text{Gpc})^3$ and the number density $n = 2 \times 10^{-4}(h^{-1}\text{Mpc})^{-3}$. Difference ratios between simulated spectra and one-loop spectra are also shown under each panel. The figure shows that their agreement becomes better after reconstruction and the perturbation works at higher k .

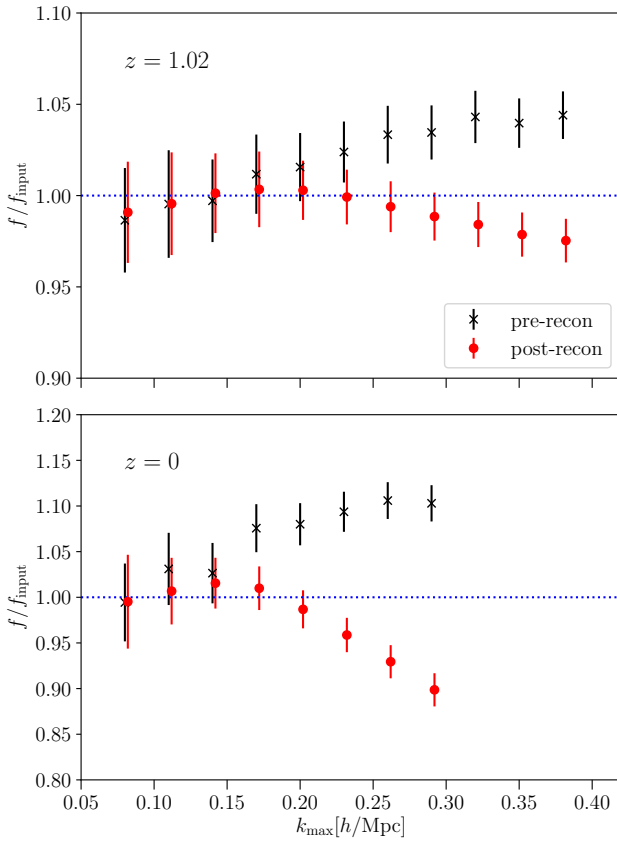


FIG. 3. Comparison of the 1σ statistical error and the systematic bias on the growth rate f expected from the monopole and quadrupole matter power spectra as a function of k_{\max} before and after reconstruction. We again assume a BOSS-like survey volume and number density, i.e., $V = 6(h^{-1}\text{Gpc})^3$ and $n = 2 \times 10^{-4}(h^{-1}\text{Mpc})^{-3}$, to compute the error of the multipole power spectra, but the output redshift is $z = 1.02$ (upper) and $z = 0$ (lower) respectively. The one-loop perturbation theory is used to fit the simulated matter power spectra and thereby the systematic error becomes significant at higher k_{\max} . The figure shows that the reconstructed spectra better reproduces the input value of f and then the systematic error exceeds the statistical error at higher k_{\max} by reconstruction.

Figure 2 shows the comparison of the monopole and quadrupole of simulated power spectrum with the one-loop perturbative formulae before (left) and after reconstruction (right) at the output redshift of 1.02 (upper) and 0 (lower). We adopt the bestfit values (the minimum χ^2) of counter terms with k_{\max} of $0.2h/\text{Mpc}$ for $z = 1$ and $0.12h/\text{Mpc}$ for $z = 0$ where the minimum χ^2 value is less than unity. In these plots, the power spectra are normalized with redshift-space no-wiggle spectrum including linear Kaiser effect [87], i.e., $P^{\text{nw},z}(k, \mu) = (1 + f\mu^2)^2 P^{\text{nw}}(k)$ where $f \equiv d \ln D(z) / d \ln a$ is the growth rate at a given z and $P^{\text{nw}}(k)$ is the no-wiggle spectrum given by Eisenstein and Hu [88]. We find that the one-loop perturbative formula can be better fitted to the post-recon spectrum up

to higher k . More quantitatively saying, k_{\max} where χ^2_{\min} becomes unity is $0.17h/\text{Mpc}$ for $z = 1$ and $0.11h/\text{Mpc}$ for $z = 0$ before reconstruction, which are extended to be $0.23h/\text{Mpc}$ for $z=1$ and $0.13h/\text{Mpc}$ for $z = 0$ after reconstruction.

We also see the impact on the measurement of the growth rate f by computing the likelihood function $\mathcal{L} \propto \exp(-\chi^2/2)$ where χ^2 is computed from the equation (30). In addition to the counter terms α_0 and α_2 , the growth rate f is treated as free parameters. Figure 3 shows the expected constraints on f from the monopole and quadrupole spectra with different k_{\max} . Here we again assume the error expected from the same BOSS-like survey volume and number density. The statistical error decreases at higher k_{\max} , however, the systematic error increases because the one-loop approximation becomes worse at higher k . We find that k_{\max} where the statistical error is comparable to the systematic one is $0.22h/\text{Mpc}$ for $z = 1$ and $0.12h/\text{Mpc}$ for $z = 0$ before reconstruction. The corresponding wavenumbers are extended to be $0.30h/\text{Mpc}$ for $z = 1$ and $0.21h/\text{Mpc}$ for $z = 0$ after reconstruction. The errors at the k_{\max} where the statistical error is comparable to the systematic one decreases from 0.0171 to 0.0128 (40% decrement) for $z = 1$ and from 0.0405 to 0.0197 (51% decrement) for $z = 0$ by reconstruction.

IV. SUMMARY AND CONCLUSIONS

We derived the one-loop perturbative formulae of the redshift-space matter power spectra after density-field reconstruction using the Zeldovich approximation. We found that the amplitudes of the one-loop nonlinear terms $P_{13}(k)$ and $P_{22}(k)$ decrease significantly in both monopole and quadrupole spectra. Our result indicates that the mode couplings among density and velocity fields associated with nonlinear gravity are partly eliminated by the reconstruction. From the comparison of N-body simulations, we showed that the one-loop perturbative formulae better describe the monopole and quadrupole of matter power spectra after reconstruction and agree with the simulated spectra at higher k . We also estimated the impact on the measurement of the growth rate when using the one-loop perturbation theory as a theoretical modeling of the redshift-space matter power spectra assuming the survey volume and number density of a BOSS-like galaxy survey. We found that the systematics due to the one-loop approximation is reduced by reconstruction and thereby the total error of the growth rate measurement including the statistical and systematic errors decreases by half.

In this paper, we focused on the redshift-space matter power spectra. We plan to extend our analysis to the power spectra of biased tracers but leave this work in the near future. In this analysis, we neglected the non-Gaussianity in the covariance of matter power spectra. Since the leading-order non-Gaussianity also comes from

the one-loop terms [89, 90], the non-Gaussianity should be smaller after reconstruction and thereby the information contents of the power spectrum is expected to increase by reconstruction. We plan to show more detailed analysis of the covariance of reconstructed power spectra in the near future.

ACKNOWLEDGMENTS

We thank Alan Heavens and Marcel Schmittfull for useful discussion. This work is supported by

MEXT/JSPS KAKENHI Grant Numbers JP16K17684 (CH), JP18H04348 (CH), JP15H05893 (RT), and JP17H01131 (RT). KK is supported by the UK STFC grant ST/N000668/1 and ST/S000550/1, and the European Research Council under the European Union's Horizon 2020 programme (grant agreement No.646702 "CosTesGrav"). Numerical computations were in part carried out on Cray XC30 and XC50 at Centre for Computational Astrophysics, National Astronomical Observatory of Japan.

Appendix A: Derivation of the one-loop matter power spectrum in redshift space

The one-loop terms of the redshift-space matter power spectra $P_{13}(k)$ and $P_{22}(k)$ are derived from the equations (27) and (28) after a lengthy but straightforward calculation. Their equations are summarized below after the integration over the azimuthal angle of \mathbf{p} as follows:

$$P_{22}^{\text{z(rec)}}(\mathbf{k}) = \sum_{n,m} \mu^{2n} f^m \frac{k^3}{4\pi^2} \int_0^\infty dr P_L(kr) \int_{-1}^1 dx P_L(k(1+r^2-2rx)^{1/2}) \frac{A_{nm}(r,x)}{(1+r^2-2rx)^2}, \quad (\text{A1})$$

and

$$P_{13}^{\text{z(rec)}}(\mathbf{k}) = (1+f\mu^2) P_L(k) \sum_{n,m} \mu^{2n} f^m \frac{k^3}{4\pi^2} \int_0^\infty dr P_0(kr) \int_{-1}^1 dx B_{nm}(r,x). \quad (\text{A2})$$

where A_{nm} and B_{nm} are the coefficients of $\mu^{2n} f^m$ terms in the one-loop terms. The reconstructed spectra depends on the smoothing kernel in the equation (8), which are used to derive the shift field from the smoothed density field, and thereby the following equations of the coefficients of the one-loop terms include $W(|\mathbf{p}|)$ and $W(|\mathbf{k} - \mathbf{p}|)$ which are denoted as W_p and W_\star respectively. These equations agree with the SPT calculation [50] at the limit of pre-reconstruction, i.e., $W_p \rightarrow 0$ and $W_\star \rightarrow 0$. The nonvanishing components of A_{nm} and B_{nm} are summarized below:

$$A_{00} = \frac{(r(7rx(W_\star - W_p) + 2(7W_p - 5)x^2 - 7W_\star + 3) - 7(W_p - 1)x)^2}{98} \quad (\text{A3})$$

$$A_{01} = -\frac{1}{14(r^2 - 2rx + 1)} [(x^2 - 1)(2r(r - x) + 1)(r(W_p x(r - 2x) - rW_\star x + W_\star) + W_p x) \\ \times (r(7rx(W_p - W_\star) + 2(5 - 7W_p)x^2 + 7W_\star - 3) + 7(W_p - 1)x)] \quad (\text{A4})$$

$$A_{11} = \frac{1}{98(r^2 - 2rx + 1)} [(r(7rx(W_\star - W_p) + 2(7W_p - 5)x^2 - 7W_\star + 3) - 7(W_p - 1)x) \\ (-14r^4 x(3x^2 - 1)(W_p - W_\star) + 2r^3(-21x^4(W_\star - 3W_p) - x^2(7W_p + 28W_\star + 20) + 7W_\star + 6) \\ + r^2 x(x^2(-91W_p + 63W_\star + 80) - 84W_p x^4 + 7W_p + 21W_\star + 4)) \\ + r(x^2(28W_p - 21W_\star - 96) + 84W_p x^4 - 7W_\star + 12) - 7x(3W_p x^2 + W_p - 4))] \quad (\text{A5})$$

$$A_{02} = \frac{3(x^2 - 1)^2}{112(r^2 - 2rx + 1)^2} [(2r^2(r^2 - 2rx + 1)(-r(W_p x(r - 2x) - rW_\star x + W_\star) - W_p x) \\ (r(7rx(W_\star - W_p) + 2(7W_p - 5)x^2 - 7W_\star + 3) - 7(W_p - 1)x) \\ + 7(2r(r - x) + 1)^2(r(W_p x(r - 2x) - rW_\star x + W_\star) + W_p x)^2)] \quad (\text{A6})$$

$$\begin{aligned}
A_{12} = & -\frac{1}{56(r^2 - 2rx + 1)^2} \left[(x^2 - 1) (126r^8x^2 (5x^2 - 1) (W_p - W_\star)^2 \right. \\
& + 2r^7x(W_p - W_\star) (30x^4(-63W_p + 21W_\star + 5) + 9x^2(14W_p + 84W_\star + 13) - 126W_\star - 1) \\
& + 2r^6 (30x^6 (133W_p^2 - 2W_p(49W_\star + 10) + W_\star(7W_\star + 10)) \\
& + 3x^4 (497W_p^2 - W_p(1624W_\star + 295) + 89W_\star(7W_\star + 3)) \\
& + x^2 (112W_pW_\star - W_p(119W_p + 111) + 574W_\star^2 + 230W_\star + 48) - 63W_\star^2 - W_\star - 6) + 4r^5x (-105W_p^2 \\
& (16x^6 + 27x^4 + x^2) + W_p (60(7W_\star + 5)x^6 + 42(84W_\star + 29)x^4 + (1498W_\star + 501)x^2 - 56W_\star + 11) \\
& - W_\star (35W_\star (9x^4 + 29x^2 + 2) + 642x^4 + 655x^2 + 68) - 96x^2 - 9) \\
& + r^4 (x^4 (5691W_p^2 - 14W_p(881W_\star + 430) + 15W_\star(91W_\star + 270) + 384) \\
& + x^2 (-63W_p^2 - 14W_p(99W_\star + 56) + W_\star(1981W_\star + 1784) + 480) \\
& + 1680W_p^2x^8 + 168W_px^6(74W_p - 25W_\star - 27) + 2(W_\star(7W_\star + 23) - 5)) \\
& + 2r^3x (-28W_p^2x^2 (60x^4 + 158x^2 + 21) + W_p (42(45W_\star + 73)x^4 + (2485W_\star + 1577)x^2 + 49W_\star + 47) \\
& - 217W_\star^2 - (W_\star(315W_\star + 1493) + 360)x^2 - 257W_\star - 88) \\
& + r^2 (x^2 (84W_p^2 - 2W_p(469W_\star + 351) + 3W_\star(35W_\star + 348) + 488) \\
& + 2520W_p^2x^6 + 2W_px^4(1512W_p - 735W_\star - 1945) + 35W_\star^2 + 48W_\star + 16) \\
& + 2rx (W_p (x^2(-252W_p + 105W_\star + 592) - 420W_px^4 + 35W_\star + 24) - 70(W_\star + 1)) \\
& \left. + 35W_px^2 (3W_px^2 + W_p - 4) + 14 \right] \tag{A7}
\end{aligned}$$

$$\begin{aligned}
A_{22} = & \frac{1}{784(r^2 - 2rx + 1)^2} \left[294r^8x^2 (35x^4 - 30x^2 + 3) (W_p - W_\star)^2 \right. \\
& + 14r^7x(W_p - W_\star) (70x^6(-63W_p + 21W_\star + 5) + x^4(2940W_p + 1050W_\star + 299) \\
& + 18x^2(7W_p - 91W_\star - 18) + 126W_\star + 11) \\
& + 2r^6 (490x^8 (133W_p^2 - 2W_p(49W_\star + 10) + W_\star(7W_\star + 10)) \\
& + x^4 (-23520W_p^2 + 14W_p(3906W_\star + 673) - 147W_\star(45W_\star + 19) + 2832) \\
& + x^2 (343W_p^2 + 133W_p(28W_\star + 13) - 7W_\star(1463W_\star + 593) - 1884) \\
& - 7x^6 ((8540W_p - 2297)W_\star + 5W_p(259W_p + 509) - 4375W_\star^2) \\
& + 441W_\star^2 + 77W_\star + 228) \\
& + 4r^5x (-7x^6 (5215W_p^2 - 2W_p(4130W_\star + 1823) + W_\star(735W_\star + 1874)) \\
& + x^4 (27146W_p^2 + 7W_p(151 - 294W_\star) - 49W_\star(344W_\star + 239) - 5664) \\
& + x^2 (3871W_p^2 - 28W_p(763W_\star + 233) + 7W_\star(1197W_\star + 850) + 1878) \\
& - 980W_px^8(28W_p - 7W_\star - 5) - 98W_pW_\star - 259W_p + 1862W_\star^2 + 1239W_\star + 258) \\
& + r^4 (x^6 (8281W_p^2 - 14W_p(14679W_\star + 8494) + 49W_\star(455W_\star + 1942) + 22656) \\
& + 2x^4 (-36701W_p^2 + 14W_p(2989W_\star + 1318) + 35W_\star(490W_\star + 293) + 13248) \\
& - 7x^2 (217W_p^2 - 2W_p(1841W_\star + 894) + W_\star(2891W_\star + 2914) + 2084) \\
& + 27440W_p^2x^{10} + 56W_px^8(3640W_p - 1225W_\star - 1699) - 14W_\star(77W_\star + 85) + 716) \\
& + 2r^3x (-392W_p^2 (70x^6 + 189x^4 - 67x^2 - 24) x^2 \\
& + 7W_p (2(2205W_\star + 5273)x^6 + (6223W_\star + 3347)x^4 - 4(847W_\star + 488)x^2 - 189W_\star - 181) \\
& - 3(245W_\star(7W_\star + 53) + 8816)x^4 - 14W_\star(301W_\star + 13)x^2 \\
& + 7W_\star(329W_\star + 551) + 592x^2 + 2336) \\
& + r^2 (-14W_\star (x^2 (7W_p (245x^4 + 190x^2 - 99) - 2124x^2 + 12) + 96) \\
& + 2x^2 (7W_p (2940W_px^6 + (3836W_p - 7381)x^4 - 98(20W_p + 3)x^2 - 112W_p + 619) \\
& + 8(2881x^2 - 680)) + 49W_\star^2 (35x^4 + 18x^2 - 5) + 64) \\
& + 14rx (-980W_p^2x^6 + W_px^4(-728W_p + 245W_\star + 2432) + 2x^2(W_p(182W_p + 63W_\star + 8) - 2(77W_\star + 317)) \\
& - 35W_pW_\star - 96W_p - 28W_\star + 260) \\
& + 49 (x^2 (W_p (35W_px^4 + 2(9W_p - 44)x^2 - 5W_p - 8) + 52) - 4) \left. \right] \tag{A8}
\end{aligned}$$

$$A_{03} = -\frac{5r^2(x^2-1)^3(2r(r-x)+1)(r(W_p x(r-2x)-rW_\star x+W_\star)+W_p x)^2}{16(r^2-2rx+1)^2} \quad (\text{A9})$$

$$\begin{aligned} A_{13} = & \frac{1}{112(r^2-2rx+1)^2} \left[3(x^2-1)^2(r(W_p x(r-2x)-rW_\star x+W_\star)+W_p x) \right. \\ & (70r^6x(7x^2-1)(W_p-W_\star)+2r^5(245x^4(W_\star-3W_p) \\ & +x^2(-105W_p+420W_\star+76)-35W_\star+8) \\ & +r^4x(x^2(1715W_p-1015W_\star-304)+980W_p x^4-7W_p-413W_\star-200) \\ & +r^3(x^2(-644W_p+693W_\star+488)-1540W_p x^4+63W_\star+58) \\ & +7r^2x(W_p(123x^2+11)-26W_\star-36) \\ & \left. +14r(-14W_p x^2+W_\star+3)+14W_p x \right] \quad (\text{A10}) \end{aligned}$$

$$\begin{aligned} A_{23} = & \frac{1}{112(r^2-2rx+1)^2} \left[(x^2-1)(-210r^8x^2(21x^4-14x^2+1)(W_p-W_\star)^2 \right. \\ & +2r^7x(W_p-W_\star)(-2205x^6(W_\star-5W_p)-10x^4(441W_p+588W_\star+116) \\ & +3x^2(-245W_p+1365W_\star+72)-210W_\star+48) \\ & +r^6(-5x^6(2989W_p^2-2W_p(5929W_\star+928)+W_\star(2989W_\star+928)) \\ & +2x^4(7245W_p^2+W_p(1240-10710W_\star)-48W_\star(105W_\star+59)) \\ & +3x^2(21W_p^2-14W_p(103W_\star+24)+W_\star(2681W_\star+416)-128) \\ & +17640W_p x^8(W_\star-2W_p)+6(16-35W_\star)W_\star+48) \\ & +2r^5x(2x^2(-1512W_p^2+21W_p(271W_\star+17)+W_\star(546W_\star+995))+384) \\ & +8820W_p^2 x^8+x^4(-21735W_p W_\star-4W_p(1645W_p+2468)+9730W_\star^2+7688W_\star) \\ & +40W_p x^6(784W_p-637W_\star-116)+3(W_p(91W_\star+54)-6W_\star(91W_\star+29)+24)) \\ & +r^4(-42140W_p^2 x^8+x^4(4(2429W_p-4894)W_\star+16(W_p(966W_p+841)-96)-12145W_\star^2) \\ & +2W_p x^6(-19390W_p+28385W_\star+13056)+14W_\star x^2(-589W_p+65W_\star-10) \\ & +8(W_p(98W_p-221)-240)x^2+3W_\star(161W_\star+76)+40) \\ & +2r^3x(x^2(-2513W_p^2+14W_p(61W_\star-98)+10W_\star(182W_\star+597)+1440)+20055W_p^2 x^6 \\ & +W_p x^4(4018W_p-15365W_\star-14208)+511W_p W_\star+180W_p-196W_\star^2-314W_\star+352) \\ & +r^2(-x^2(-539W_p^2+8W_p(105W_\star+46)+12W_\star(35W_\star+291)+1952) \\ & -19005W_p^2 x^6+2W_p x^4(413W_p+4060W_\star+7520)+4W_\star(7W_\star+33)-64) \\ & +4rx(W_p(-x^2(112W_p+210W_\star+971)+1120W_p x^4+14W_\star+33)+98W_\star+140) \\ & \left. +28W_p x^2(-15W_p x^2+W_p+14)-56 \right] \quad (\text{A11}) \end{aligned}$$

$$\begin{aligned}
A_{33} = & \frac{1}{112(r^2 - 2rx + 1)^2} \left[14r^8x^2 (21x^2 (11x^4 - 15x^2 + 5) - 5) (W_p - W_\star)^2 \right. \\
& + 2r^7x(W_p - W_\star) (1617x^8(W_\star - 5W_p) + 21x^6(399W_p + 175W_\star + 52) - 5x^4(147W_p + 1323W_\star + 176) \\
& + x^2(-455W_p + 2065W_\star - 12) - 70W_\star + 24) \\
& + r^6 (-21x^8 (119W_p^2 + 2W_p(945W_\star + 208) - W_\star(553W_\star + 208)) \\
& + x^6 (-23275W_p^2 + W_p(47726W_\star + 2248) + W_\star(2303W_\star + 3456)) \\
& + x^4 (6055W_p^2 + W_p(3664 - 2030W_\star) - 21W_\star(695W_\star + 256) + 704) \\
& + x^2 (119W_p^2 - 6W_p(413W_\star + 52) + W_\star(4109W_\star + 192) - 528) \\
& - 12936W_p x^{10} (W_\star - 2W_p) - 70W_\star^2 + 48W_\star + 48) \\
& + 2r^5x (x^6 (20776W_p^2 + W_p(8379W_\star + 8248) - 2W_\star(4067W_\star + 4034)) \\
& + x^4 (2660W_p^2 - W_p(24745W_\star + 7297) + W_\star(3094W_\star + 2165) - 1408) \\
& - 6468W_p^2 x^{10} + x^2 (4025W_p W_\star - 2W_p(742W_p + 333) + 3654W_\star^2 + 2678W_\star + 616) \\
& - 84W_p x^8 (259W_p - 238W_\star - 52) + 189W_p W_\star + 51W_p - 854W_\star^2 - 135W_\star + 120) \\
& + r^4 (x^6 (-39130W_p^2 + 2W_p(7329W_\star - 724) + W_\star(11123W_\star + 23148) + 2816) \\
& + x^4 (3612W_p^2 + 6W_p(3591W_\star + 2308) - W_\star(6307W_\star + 12354) + 2816) \\
& - x^2 (-434W_p^2 + 2W_p(1785W_\star + 88) + W_\star(1715W_\star + 1888) + 2312) \\
& + 33516W_p^2 x^{10} + 2W_p x^8 (8624W_p - 24157W_\star - 13952) + 259W_\star^2 + 54W_\star + 40) \\
& + 2r^3x (x^4 (7455W_p^2 - W_p(7749W_\star + 7178) - W_\star(1862W_\star + 8065) - 3168) \\
& + x^2 (-917W_p^2 - W_p(2149W_\star + 2276) + 14W_\star(78W_\star + 331) + 480) \\
& - 17395W_p^2 x^8 + W_p x^6 (4585W_p + 14357W_\star + 17264) + 245W_p W_\star + 30W_p + 98W_\star^2 + 71W_\star + 448) \\
& + r^2 (x^4 (-2597W_p^2 + 8W_p(609W_\star + 1382) + 490W_\star^2 + 5478W_\star + 5344) \\
& + x^2 (231W_p^2 + W_p(420W_\star + 416) - 12(W_\star(21W_\star + 233) + 160)) \\
& + 18081W_p^2 x^8 - W_p x^6 (9443W_p + 8428W_\star + 20880) + 2(3 - 7W_\star)W_\star - 64) \\
& + 2rx (2x^2 (56W_p^2 - 14(9W_p + 13)W_\star - 769W_p - 500) \\
& - 2352W_p^2 x^6 + W_p x^4 (1344W_p + 490W_\star + 3103) - 14W_p W_\star + 3W_p + 140W_\star + 328) \\
& \left. + 14x^2 (W_p (35W_p x^4 - 2(9W_p + 26)x^2 - W_p + 20) + 20) - 56 \right] \tag{A12}
\end{aligned}$$

$$A_{04} = \frac{35r^4 (x^2 - 1)^4 (r(W_p x(r - 2x) - rW_\star x + W_\star) + W_p x)^2}{256 (r^2 - 2rx + 1)^2} \quad (\text{A13})$$

$$\begin{aligned} A_{14} = & -\frac{1}{64 (r^2 - 2rx + 1)^2} \\ & \left[5r^2 (x^2 - 1)^3 (r(W_p x(r - 2x) - rW_\star x + W_\star) + W_p x) (7r^4 x (9x^2 - 1) (W_p - W_\star) \right. \\ & + r^3 (-42W_p (3x^4 + x^2) + 7W_\star (17x^2 - 1) + 4) \\ & \left. + r^2 x (5W_p (35x^2 + 1) - 68W_\star - 8) + 4r (-20W_p x^2 + 3W_\star + 1) + 12W_p x) \right] \end{aligned} \quad (\text{A14})$$

$$\begin{aligned} A_{24} = & \frac{1}{128 (r^2 - 2rx + 1)^2} \left[3 (x^2 - 1)^2 (35r^8 x^2 (33x^4 - 18x^2 + 1) (W_p - W_\star)^2 \right. \\ & + 10r^7 x (W_p - W_\star) (21x^4 (4W_p + 19W_\star) + 14x^2 (3W_p - 13W_\star + 2) - 462W_p x^6 + 7W_\star - 4) \\ & + r^6 (5 (924W_p^2 x^8 + 7x^4 (4(7W_p + 4)W_\star - 8W_p (9W_p + 4) + 153W_\star^2) \\ & + 42W_p x^6 (31W_p - 65W_\star) + 2W_\star x^2 (115W_p - 187W_\star + 44) \\ & + W_\star (7W_\star - 8)) - 10W_p (5W_p + 8)x^2 + 8) \\ & + 2r^5 x (10x^2 (65W_p^2 + W_p (68 - 155W_\star) - 22W_\star (8W_\star + 3)) \\ & - 5670W_p^2 x^6 + 35W_p x^4 (-28W_p + 225W_\star + 16) - 85W_p W_\star - 16W_p + 400W_\star^2 - 84W_\star - 16) \\ & + r^4 (x^2 (-197W_p^2 + 32W_p (47W_\star - 16) + 8W_\star (146W_\star + 137) + 32) \\ & + 11235W_p^2 x^6 - 10W_p x^4 (103W_p + 904W_\star + 208) + 8 (-15W_\star^2 + W_\star + 2)) \\ & + 8r^3 x (-710W_p^2 x^4 + W_p x^2 (86W_p + 334W_\star + 179) - 28W_p W_\star + 7W_p - 22W_\star^2 - 48W_\star - 4) \\ & + 8r^2 (189W_p^2 x^4 - W_p x^2 (13W_p + 46W_\star + 54) + W_\star^2 + 6W_\star + 1) \\ & \left. + 16rW_p x (-12W_p x^2 + W_\star + 3) + 8W_p^2 x^2) \right] \end{aligned} \quad (\text{A15})$$

$$\begin{aligned} A_{34} = & -\frac{1}{64 (r^2 - 2rx + 1)^2} \left[(x^2 - 1) (7r^8 x^2 (429x^6 - 495x^4 + 135x^2 - 5) (W_p - W_\star)^2 \right. \\ & + 2r^7 x (W_p - W_\star) (231x^6 (18W_p + 25W_\star) + 315x^4 (2W_p - 19W_\star + 2) - 35x^2 (10W_p - 39W_\star + 12) \\ & - 6006W_p x^8 - 35W_\star + 30) + r^6 (35x^4 (74W_p^2 + 6W_p (29W_\star + 8) + 9(4 - 51W_\star)W_\star) \\ & + 5x^2 (22W_p^2 + W_p (96 - 366W_\star) + 3W_\star (187W_\star - 96) + 24) + 12012W_p^2 x^{10} \\ & + 21x^6 (6(177W_p + 20)W_\star - 30W_p (31W_p + 8) + 851W_\star^2) + 462W_p x^8 (31W_p - 87W_\star) \\ & - 35W_\star^2 + 60W_\star - 24) + 2r^5 x (7x^4 (850W_p^2 + 5W_p (84 - 535W_\star) \\ & - 2W_\star (508W_\star + 255)) - 17094W_p^2 x^8 \\ & + 5x^2 (3(55W_p + 52)W_\star - 2W_p (89W_p + 180) + 1056W_\star^2 - 48) \\ & + 21W_p x^6 (186W_p + 1295W_\star + 120) + 145W_p W_\star - 12W_p - 600W_\star^2 + 342W_\star) \\ & + r^4 (5x^4 (-363W_p^2 + 4928W_p W_\star + 4W_\star (307W_\star + 387) + 96) + 40299W_p^2 x^8 \\ & - 7W_p x^6 (3095W_p + 5464W_\star + 1680) - 24W_\star x^2 (73W_p + 146W_\star + 103) \\ & + (7W_p (43W_p + 240) + 528)x^2 \\ & + 12W_\star (15W_\star - 7) - 32) + 4r^3 x (-2x^2 (63W_p^2 + W_p (972W_\star + 309) + 2W_\star (85W_\star + 252) + 108) \\ & - 6286W_p^2 x^6 + 5W_p x^4 (716W_p + 738W_\star + 543) + 78W_p W_\star - 57W_p + 132W_\star^2 + 264W_\star - 40) \\ & + 4r^2 (x^2 (33W_p^2 + 276W_p (W_\star + 1) + 6W_\star (5W_\star + 42) + 142) \\ & + 2185W_p^2 x^6 - 2W_p x^4 (537W_p + 370W_\star + 618) - 6W_\star (W_\star + 6) + 2) \\ & + 16rx (W_p (3x^2 (12W_p + 5W_\star + 23) - 100W_p x^4 - 3(W_\star + 3)) - 2(3W_\star + 5)) \\ & \left. + 24W_p x^2 (W_p (5x^2 - 1) - 4) + 16) \right] \end{aligned} \quad (\text{A16})$$

$$\begin{aligned}
A_{44} = & \frac{1}{256(r^2 - 2rx + 1)^2} \left[(W_p - W_*)^2 x^2 (6435x^8 - 12012x^6 + 6930x^4 - 1260x^2 + 35) \right. \\
& r^8 + 2(W_p - W_*)x (-12870W_p x^{10} + 429(40W_p + 31W_*)x^8 - 924(3W_p + 25W_* - 2)x^6 \\
& - 630(4W_p - 19W_* + 4)x^4 + 70(7W_p - 26W_* + 12)x^2 + 5(7W_* - 8))r^7 \\
& + (25740W_p^2 x^{12} + 858W_p(23W_p - 109W_*)x^{10} \\
& + 33(1363W_*^2 + 8(421W_p + 28)W_* - 448W_p(5W_p + 1))x^8 \\
& + 84(405W_p^2 + (168 - 87W_*)W_p - W_*(851W_* + 4))x^6 \\
& - 70(26W_p^2 + 260W_*W_p + 3(40 - 153W_*)W_* - 8)x^4 \\
& - 10(374W_*^2 - 251W_pW_* - 296W_* + W_p(17W_p + 112) + 48)x^2 + 35W_*^2 - 80W_* + 48)r^6 \\
& + 2x(-40326W_p^2 x^{10} + 33W_p(984W_p + 2115W_* + 224)x^8 \\
& + 12(1365W_p^2 + (476 - 7805W_*)W_p - 2W_*(832W_* + 483))x^6 \\
& - 14(940W_p^2 + (960 - 1975W_*)W_p - 4W_*(508W_* + 171) + 80)x^4 \\
& + 10(105W_p^2 + (90W_* + 296)W_p + 12(7 - 88W_*)W_* + 64)x^2 \\
& + 800W_*^2 + 64W_p - 205W_pW_* - 744W_* + 96)r^5 \\
& + (105699W_p^2 x^{10} - 12W_p(10241W_p + 9176W_* + 3248)x^8 + 14(1415W_p^2 + 96(107W_* + 16)W_p \\
& + 8W_*(176W_* + 255) + 160)x^6 + 20(337W_p^2 + 8(74 - 277W_*)W_p - 4W_*(307W_* + 337) + 88)x^4 \\
& + (-397W_p^2 + 1664(W_* - 2)W_p + 48(W_*(146W_* + 69) - 44))x^2 - 16(W_* - 1)(15W_* + 2))r^4 \\
& + 16x(-4638W_p^2 x^8 + 7W_p(806W_p + 434W_* + 369)x^6 \\
& - (322W_*^2 + 4(905W_p + 272)W_* + 5W_p(290W_p + 427) + 300)x^4 \\
& + (-2W_p^2 + (942W_* + 81)W_p + 4W_*(85W_* + 242) + 88)x^2 \\
& - 66W_*^2 + 31W_p - 24W_pW_* - 120W_* + 52)r^3 \\
& + 16(1841W_p^2 x^8 - W_p(2115W_p + 714W_* + 1378)x^6 \\
& + (507W_p^2 + 4(185W_* + 289)W_p + 5W_*(7W_* + 66) + 243)x^4 \\
& - (3W_p(3W_p + 38) + 118)x^2 - 6W_*(23W_p + 5W_* + 42)x^2 + 3W_*(W_* + 6) - 5)r^2 \\
& + 32x(-196W_p^2 x^6 + 5W_p(40W_p + 7W_* + 37)x^4 - 2(10W_* + 3W_p(6W_p + 5W_* + 23) + 22)x^2 \\
& + 9W_p + 3W_pW_* + 12W_* + 20)r + 16(35W_p^2 x^6 - 10W_p(3W_p + 4)x^4 + 3(W_p(W_p + 8) + 4)x^2 - 4)] \tag{A17}
\end{aligned}$$

and

$$\begin{aligned}
B_{00} = & \frac{1}{7(r^2 - 2rx + 1)} \left[2rx^3 (7W_p(-2r^2 + W - 2) + 4r^2W_*) \right. \\
& + x^2 (7(r^2 + 1)W_p(2r^2 - W + 2) - 2r^2(7r^2 + 11)W_*) \\
& \left. + 2r(17r^2 + 7)W_*x - 20r^2W_* \right] \tag{A18}
\end{aligned}$$

$$\begin{aligned}
B_{01} = & \frac{1}{7(r^2 - 2rx + 1)^2(r^2 + 2rx + 1)} \left[(x^2 - 1)(4r^2(r^2 + 1)x^4(W_p(11r^2 - 7W + 7) - 11r^2W_*) \right. \\
& + r^2(r^2 + 1)(23r^2 + 17)W_* + 8r^3x^5(W_p(-11r^2 + 7W - 7) + 2r^2W_*) \\
& + x^2 \left(7(r^2 + 1)^3W_p^2 - (14r^6 + 23r^4 + 28r^2 + 7)(r^2 + 1)W_p + r^2(14r^6 + 21r^4 - 38r^2 + 11)W_* \right) \\
& + 2rx^3 \left((r^4 + 55r^2 + 12)r^2W_* + W_p(14r^6 + 23r^4 - 7(r^2 + 1)^2W_p + 28r^2 + 7) \right) \\
& \left. - r(37r^6 + 63r^4 + 45r^2 + 7)W_*x \right] \tag{A19}
\end{aligned}$$

$$\begin{aligned}
B_{11} = & \frac{3}{7(r^2 - 2rx + 1)^2(r^2 + 2rx + 1)} [4r^2(r^2 + 1)x^6(W_p(-11r^2 + 7W - 7) + 11r^2W_\star) \\
& + x^2((r^2 + 1)(19r^4 + 14r^2 + 7)W - 4r^2(13r^4 + 14r^2 + 7)W_\star) \\
& + 3r^2(r^4 - 1)W_\star + 8r^3x^7(W_p(11r^2 - 7W + 7) - 2r^2W_\star) \\
& - 2rx^5((r^4 + 63r^2 + 12)r^2W_\star + W_p(14r^6 + 11r^4 - 7(r^2 + 1)^2W + 7)) \\
& + x^4((r^2 + 1)W_p(14r^6 + 11r^4 - 7(r^2 + 1)^2W + 7) - r^2(14r^6 + 9r^4 - 82r^2 + 11)W_\star) \\
& + rx^3((47r^6 + 53r^4 + 21r^2 + 7)W_\star - 2(19r^4 + 14r^2 + 7)W) \\
& + r(-3r^6 + 19r^4 + 17r^2 + 7)W_\star x] \tag{A20}
\end{aligned}$$

$$\begin{aligned}
B_{02} = & \frac{3}{56(r^2 - 2rx + 1)^2(r^2 + 2rx + 1)} [(x^2 - 1)^2(-2r^2(r^2 + 1)(13r^2 + 7)W_\star \\
& + 4r^2x^4(8r^4W_\star - (r^2 + 1)W_p(8r^2 - 7W))) \\
& - 2rx^3(W_p(2r^2(7r^4 + 2r^2 + 7) - 7(r^2 + 1)^2W_p) + 2(3r^2 + 25)r^4W_\star) \\
& + 8r^3W_p x^5(8r^2 - 7W) + x^2(2(-7r^4 + 4r^2 + 27)r^4W_\star \\
& + W_p(2r^2(7r^6 + 9r^4 + 9r^2 + 7) - 7(r^2 + 1)^3W_p)) + 4r^3(10r^4 + 11r^2 + 7)W_\star x)] \tag{A21}
\end{aligned}$$

$$\begin{aligned}
B_{12} = & \frac{1}{28(r^2 - 2rx + 1)^2(r^2 + 2rx + 1)} [(x^2 - 1)(6r^2(r^2 + 1)(r^2 + 11)W_\star \\
& + 60r^2x^6((r^2 + 1)W_p(8r^2 - 7W_p) - 8r^4W_\star) + 120r^3W_p x^7(7W_p - 8r^2) + 2rx^5(30r^6(7W_p + 3W_\star) \\
& + 3r^4(314W_\star - 5W_p(7W_p + 44)) - 2r^2W_p(91W_p + 167) - 105W_p^2) \\
& + 2rx^3(-7(r^2 + 1)^2W_p^2 - 2(201r^4 - 42r^2 + 5)r^2W_\star + 2(63r^6 + 290r^4 + 223r^2 + 56)W_p) \\
& + x^2(7(r^2 + 1)^3W_p^2 - 2(63r^6 + 290r^4 + 223r^2 + 56)(r^2 + 1)W_p \\
& + 2r^2(63r^6 + 587r^4 + 469r^2 + 233)W_\star) + x^4(2r^4(105r^2(r^2 - 4) - 869)W_\star \\
& - (r^2 + 1)W_p(210r^6 - 15r^4(7W_p + 44) - 2r^2(91W_p + 167) - 105W_p)) \\
& - 4r(33r^6 + 163r^4 + 128r^2 + 28)W_\star x)] \tag{A22}
\end{aligned}$$

$$\begin{aligned}
B_{22} = & \frac{1}{56} \left[\frac{1}{r^4 + r^2(2 - 4x^2) + 1} \right. \\
& \times (2W_p x^2(7r^6(35x^4 + 10x^2 - 21) - 2r^4(280x^6 + 405x^4 - 866x^2 + 265) \\
& + r^2(-747x^4 + 934x^2 - 355) + 56(4x^2 - 1)) \\
& - \frac{1}{(r^2 - 2rx + 1)^2}(2rW_\star(rx - 1)(7r^4x(35x^4 + 10x^2 - 21) + r^3(-280x^6 - 1055x^4 + 618x^2 + 45) \\
& + r^2x(1055x^4 + 426x^2 - 473) + r(-901x^4 + 142x^2 + 87) + 56x(4x^2 - 1))) \\
& \left. + 7W_p^2(-35x^4 + 6x^2 + 5)x^2 \right] \tag{A23}
\end{aligned}$$

$$\begin{aligned}
B_{13} = & -\frac{3}{8(r^2 - 2rx + 1)} [(x^2 - 1)^2(-14r^3W_\star x + 2rW_p x^3(10r^2 - W) + 4r^2W_\star \\
& + x^2(10r^4(W_\star - W) + r^2(W - 10)W + W_p^2))] \tag{A24}
\end{aligned}$$

$$\begin{aligned}
B_{23} = & -\frac{1}{4(r^2 - 2rx + 1)} [-3(5x^4 - 6x^2 + 1)(W_p^2 x^2(r^2 - 2rx + 1) - 4r^2W_\star(rx - 1)) \\
& + 10r^2x(7x^4 - 10x^2 + 3)(r(W_p x(r - 2x) - rW_\star x + W_\star) + W_p x) \\
& - 12x(1 - x^2)(r(W_p x(r - 2x) - rW_\star x + W_\star) + W_p x)] \tag{A25}
\end{aligned}$$

$$\begin{aligned}
B_{33} = & -\frac{1}{8(r^2 - 2rx + 1)} [(35x^4 - 30x^2 + 3)(W_p^2 x^2(r^2 - 2rx + 1) - 4r^2W_\star(rx - 1)) \\
& - 2r^2x(63x^4 - 70x^2 + 15)(r(W_p x(r - 2x) - rW_\star x + W_\star) + W_p x) \\
& + 8x(3 - 5x^2)(r(W_p x(r - 2x) - rW_\star x + W_\star) + W_p x)] \tag{A26}
\end{aligned}$$

-
- [1] L. Amendola, C. Quercellini, and E. Giallongo, MNRAS **357**, 429 (2005), astro-ph/0404599.
- [2] D. J. Eisenstein, W. Hu, and M. Tegmark, ApJ **504**, L57 (1998), astro-ph/9805239.
- [3] A. Meiksin, M. White, and J. A. Peacock, MNRAS **304**, 851 (1999), astro-ph/9812214.
- [4] C. Blake and K. Glazebrook, Astrophys. J. **594**, 665 (2003), astro-ph/0301632.
- [5] W. Hu and Z. Haiman, Phys. Rev. D **68**, 063004 (2003), astro-ph/0306053.
- [6] T. Matsubara, Astrophys. J. **615**, 573 (2004), astro-ph/0408349.
- [7] R. E. Angulo, C. M. Baugh, C. S. Frenk, R. G. Bower, A. Jenkins, and S. L. Morris, MNRAS **362**, L25 (2005), astro-ph/0504456.
- [8] H.-J. Seo and D. J. Eisenstein, Astrophys. J. **633**, 575 (2005), astro-ph/0507338.
- [9] M. White, Astroparticle Physics **24**, 334 (2005), astro-ph/0507307.
- [10] D. J. Eisenstein, H.-J. Seo, and M. White, Astrophys. J. **664**, 660 (2007), astro-ph/0604361.
- [11] E. Huff, A. E. Schulz, M. White, D. J. Schlegel, and M. S. Warren, Astroparticle Physics **26**, 351 (2007), astro-ph/0607061.
- [12] R. E. Angulo, C. M. Baugh, C. S. Frenk, and C. G. Lacey, MNRAS **383**, 755 (2008), astro-ph/0702543.
- [13] D. J. Eisenstein, I. Zehavi, D. W. Hogg, R. Scoccimarro, M. R. Blanton, R. C. Nichol, R. Scranton, H.-J. Seo, M. Tegmark, Z. Zheng, et al., Astrophys. J. **633**, 560 (2005), astro-ph/0501171.
- [14] S. Cole, W. J. Percival, J. A. Peacock, P. Norberg, C. M. Baugh, C. S. Frenk, I. Baldry, J. Bland-Hawthorn, T. Bridges, R. Cannon, et al., MNRAS **362**, 505 (2005), astro-ph/0501174.
- [15] N. Padmanabhan, D. J. Schlegel, U. Seljak, A. Makarov, N. A. Bahcall, M. R. Blanton, J. Brinkmann, D. J. Eisenstein, D. P. Finkbeiner, J. E. Gunn, et al., MNRAS **378**, 852 (2007), astro-ph/0605302.
- [16] W. J. Percival, R. C. Nichol, D. J. Eisenstein, J. A. Frieman, M. Fukugita, J. Loveday, A. C. Pope, D. P. Schneider, A. S. Szalay, M. Tegmark, et al., Astrophys. J. **657**, 645 (2007), astro-ph/0608636.
- [17] T. Okumura, T. Matsubara, D. J. Eisenstein, I. Kayo, C. Hikage, A. S. Szalay, and D. P. Schneider, Astrophys. J. **676**, 889 (2008), 0711.3640.
- [18] X. Xu, A. J. Cuesta, N. Padmanabhan, D. J. Eisenstein, and C. K. McBride, MNRAS **431**, 2834 (2013), 1206.6732.
- [19] L. Anderson, É. Aubourg, S. Bailey, F. Beutler, V. Bhardwaj, M. Blanton, A. S. Bolton, J. Brinkmann, J. R. Brownstein, A. Burden, et al., MNRAS **441**, 24 (2014), 1312.4877.
- [20] R. Tojeiro, A. J. Ross, A. Burden, L. Samushia, M. Manera, W. J. Percival, F. Beutler, J. Brinkmann, J. R. Brownstein, A. J. Cuesta, et al., MNRAS **440**, 2222 (2014), 1401.1768.
- [21] E. A. Kazin, J. Koda, C. Blake, N. Padmanabhan, S. Brough, M. Colless, C. Contreras, W. Couch, S. Croom, D. J. Croton, et al., MNRAS **441**, 3524 (2014), 1401.0358.
- [22] A. J. Ross, L. Samushia, C. Howlett, W. J. Percival, A. Burden, and M. Manera, MNRAS **449**, 835 (2015), 1409.3242.
- [23] S. Alam, M. Ata, S. Bailey, F. Beutler, D. Bizyaev, J. A. Blazek, A. S. Bolton, J. R. Brownstein, A. Burden, C.-H. Chuang, et al., ArXiv e-prints (2016), 1607.03155.
- [24] F. Beutler, H.-J. Seo, A. J. Ross, P. McDonald, S. Saito, A. S. Bolton, J. R. Brownstein, C.-H. Chuang, A. J. Cuesta, D. J. Eisenstein, et al., MNRAS **464**, 3409 (2017), 1607.03149.
- [25] M. Takada, E. Komatsu, and T. Futamase, Phys. Rev. D **73**, 083520 (2006), astro-ph/0512374.
- [26] S. Saito, M. Takada, and A. Taruya, Phys. Rev. D **83**, 043529 (2011), 1006.4845.
- [27] L. Guzzo, M. Pierleoni, B. Meneux, E. Branchini, O. Le Fèvre, C. Marinoni, B. Garilli, J. Blaizot, G. De Lucia, A. Pollo, et al., Nature (London) **451**, 541 (2008), 0802.1944.
- [28] K. Yamamoto, T. Sato, and G. Hütsi, Progress of Theoretical Physics **120**, 609 (2008), 0805.4789.
- [29] B. A. Reid, L. Samushia, M. White, W. J. Percival, M. Manera, N. Padmanabhan, A. J. Ross, A. G. Sánchez, S. Bailey, D. Bizyaev, et al., MNRAS **426**, 2719 (2012), 1203.6641.
- [30] F. Beutler, S. Saito, H.-J. Seo, J. Brinkmann, K. S. Dawson, D. J. Eisenstein, A. Font-Ribera, S. Ho, C. K. McBride, F. Montesano, et al., ArXiv e-prints (2013), 1312.4611.
- [31] L. Samushia, B. A. Reid, M. White, W. J. Percival, A. J. Cuesta, G.-B. Zhao, A. J. Ross, M. Manera, É. Aubourg, F. Beutler, et al., ArXiv e-prints (2013), 1312.4899.
- [32] A. Oka, S. Saito, T. Nishimichi, A. Taruya, and K. Yamamoto, ArXiv e-prints (2013), 1310.2820.
- [33] C. Hikage and K. Yamamoto, JCAP **8**, 019 (2013), 1303.3380.
- [34] M. Takada, R. Ellis, M. Chiba, J. E. Greene, H. Aihara, N. Arimoto, K. Bundy, J. Cohen, O. Doré, G. Graves, et al., ArXiv e-prints (2012), 1206.0737.
- [35] DESI Collaboration, A. Aghamousa, J. Aguilar, S. Ahlen, S. Alam, L. E. Allen, C. Allende Prieto, J. Annis, S. Bailey, C. Balland, et al., ArXiv e-prints (2016), 1611.00036.
- [36] G. J. Hill, K. Gebhardt, E. Komatsu, N. Drory, P. J. MacQueen, J. Adams, G. A. Blanc, R. Koehler, M. Rafal, M. M. Roth, et al., in *Panoramic Views of Galaxy Formation and Evolution*, edited by T. Kodama, T. Yamada, and K. Aoki (2008), vol. 399 of *Astronomical Society of the Pacific Conference Series*, p. 115, 0806.0183.
- [37] L. Amendola, S. Appleby, A. Avgoustidis, D. Bacon, T. Baker, M. Baldi, N. Bartolo, A. Blanchard, C. Bonvin, S. Borgani, et al., ArXiv e-prints (2016), 1606.00180.
- [38] D. Spergel, N. Gehrels, C. Baltay, D. Bennett, J. Breckinridge, M. Donahue, A. Dressler, B. S. Gaudi, T. Greene, O. Guyon, et al., ArXiv e-prints (2015), 1503.03757.
- [39] M. Crocce and R. Scoccimarro, Phys. Rev. D **77**, 023533 (2008), 0704.2783.
- [40] E. T. Vishniac, MNRAS **203**, 345 (1983).
- [41] J. N. Fry, Astrophys. J. **279**, 499 (1984).
- [42] M. H. Goroff, B. Grinstein, S.-J. Rey, and M. B. Wise, Astrophys. J. **311**, 6 (1986).
- [43] Y. Suto and M. Sasaki, Physical Review Letters **66**, 264 (1991).

- [44] N. Makino, M. Sasaki, and Y. Suto, Phys. Rev. D **46**, 585 (1992).
- [45] B. Jain and E. Bertschinger, Astrophys. J. **431**, 495 (1994), astro-ph/9311070.
- [46] F. R. Bouchet, S. Colombi, E. Hivon, and R. Juszkiewicz, A&Ap. **296**, 575 (1995), astro-ph/9406013.
- [47] R. Scoccimarro and J. A. Frieman, Astrophys. J. **473**, 620 (1996), astro-ph/9602070.
- [48] F. Bernardeau, S. Colombi, E. Gaztañaga, and R. Scoccimarro, Physics Report **367**, 1 (2002), astro-ph/0112551.
- [49] D. Jeong and E. Komatsu, Astrophys. J. **651**, 619 (2006), astro-ph/0604075.
- [50] T. Matsubara, Phys. Rev. D **77**, 063530 (2008), 0711.2521.
- [51] T. Matsubara, Phys. Rev. D **78**, 083519 (2008), 0807.1733.
- [52] A. Taruya, T. Nishimichi, and S. Saito, Phys. Rev. D **82**, 063522 (2010), 1006.0699.
- [53] T. Nishimichi and A. Taruya, Phys. Rev. D **84**, 043526 (2011).
- [54] A. Taruya, F. Bernardeau, T. Nishimichi, and S. Codis, Phys. Rev. D **86**, 103528 (2012), 1208.1191.
- [55] P. Valageas, T. Nishimichi, and A. Taruya, Phys. Rev. D **87**, 083522 (2013), 1302.4533.
- [56] D. J. Eisenstein, H.-J. Seo, E. Sirk, and D. N. Spergel, Astrophys. J. **664**, 675 (2007), astro-ph/0604362.
- [57] Y. B. Zel'dovich, A&Ap. **5**, 84 (1970).
- [58] H.-J. Seo, E. R. Siegel, D. J. Eisenstein, and M. White, Astrophys. J. **686**, 13 (2008), 0805.0117.
- [59] N. Padmanabhan, M. White, and J. D. Cohn, Phys. Rev. D **79**, 063523 (2009), 0812.2905.
- [60] Y. Noh, M. White, and N. Padmanabhan, Phys. Rev. D **80**, 123501 (2009), 0909.1802.
- [61] H.-J. Seo, J. Eckel, D. J. Eisenstein, K. Mehta, M. Metchnik, N. Padmanabhan, P. Pinto, R. Takahashi, M. White, and X. Xu, Astrophys. J. **720**, 1650 (2010), 0910.5005.
- [62] B. D. Sherwin and M. Zaldarriaga, Phys. Rev. D **85**, 103523 (2012), 1202.3998.
- [63] N. Padmanabhan, X. Xu, D. J. Eisenstein, R. Scalzo, A. J. Cuesta, K. T. Mehta, and E. Kazin, MNRAS **427**, 2132 (2012), 1202.0090.
- [64] S. Tashev and M. Zaldarriaga, JCAP **2012**, 006 (2012), 1203.6066.
- [65] M. Schmittfull, Y. Feng, F. Beutler, B. Sherwin, and M. Y. Chu, Phys. Rev. D **92**, 123522 (2015), 1508.06972.
- [66] H.-J. Seo, F. Beutler, A. J. Ross, and S. Saito, MNRAS **460**, 2453 (2016), 1511.00663.
- [67] M. Schmittfull, T. Baldauf, and M. Zaldarriaga, Phys. Rev. D **96**, 023505 (2017), 1704.06634.
- [68] X. Wang, H.-R. Yu, H.-M. Zhu, Y. Yu, Q. Pan, and U.-L. Pen, ApJ **841**, L29 (2017), 1703.09742.
- [69] Y. Yu, H.-M. Zhu, and U.-L. Pen, Astrophys. J. **847**, 110 (2017), 1703.08301.
- [70] R. Hada and D. J. Eisenstein, MNRAS **478**, 1866 (2018), 1804.04738.
- [71] S.-F. Chen, Z. Vlah, and M. White, arXiv e-prints arXiv:1907.00043 (2019), 1907.00043.
- [72] F. Bernardeau, Astrophys. J. **433**, 1 (1994), astro-ph/9312026.
- [73] P. Fosalba and E. Gaztanaga, MNRAS **301**, 503 (1998), astro-ph/9712095.
- [74] R. Takahashi, Progress of Theoretical Physics **120**, 549 (2008), 0806.1437.
- [75] B. Bose and K. Koyama, JCAP **2016**, 032 (2016), 1606.02520.
- [76] C. Hikage, K. Koyama, and A. Heavens, Phys. Rev. D **96**, 043513 (2017), 1703.07878.
- [77] A. F. Heavens, S. Matarrese, and L. Verde, MNRAS **301**, 797 (1998), astro-ph/9808016.
- [78] R. Scoccimarro, H. M. P. Couchman, and J. A. Frieman, Astrophys. J. **517**, 531 (1999), astro-ph/9808305.
- [79] V. Springel, MNRAS **364**, 1105 (2005), astro-ph/0505010.
- [80] M. Crocce, S. Pueblas, and R. Scoccimarro, MNRAS **373**, 369 (2006), astro-ph/0606505.
- [81] T. Nishimichi, A. Shirata, A. Taruya, K. Yahata, S. Saito, Y. Suto, R. Takahashi, N. Yoshida, T. Matsubara, N. Sugiyama, et al., PASJ **61**, 321 (2009), 0810.0813.
- [82] A. Lewis, A. Challinor, and A. Lasenby, Astrophys. J. **538**, 473 (2000), astro-ph/9911177.
- [83] Note1, FFTW3 at <http://www.fftw.org>.
- [84] Planck Collaboration, P. A. R. Ade, N. Aghanim, M. Arnaud, M. Ashdown, J. Aumont, C. Baccigalupi, A. J. Banday, R. B. Barreiro, J. G. Bartlett, et al., A&Ap. **594**, A13 (2016), 1502.01589.
- [85] J. J. M. Carrasco, M. P. Hertzberg, and L. Senatore, Journal of High Energy Physics **9**, 82 (2012), 1206.2926.
- [86] L. Fonseca de la Bella, D. Regan, D. Seery, and S. Hotchkiss, JCAP **2017**, 039 (2017), 1704.05309.
- [87] N. Kaiser, MNRAS **227**, 1 (1987).
- [88] D. J. Eisenstein and W. Hu, Astrophys. J. **496**, 605 (1998), astro-ph/9709112.
- [89] I. Mohammed, U. Seljak, and Z. Vlah, MNRAS **466**, 780 (2017), 1607.00043.
- [90] D. Wadekar and R. Scoccimarro, arXiv e-prints arXiv:1910.02914 (2019), 1910.02914.